Molecular Cell
Article

PDZ Domains of Par-3 as Potential Phosphoinositide Signaling Integrators

Hao Wu,[1,2] Wei Feng,[1,2] Jia Chen,[1] Ling-Nga Chan,[1] Siyi Huang,[1] and Mingjie Zhang[1,*]
[1]Department of Biochemistry, Molecular Neuroscience Center, The Hong Kong University of Science and Technology, Clear Water Bay, Kowloon, Hong Kong, P.R. China
[2]These authors contributed equally to this work.
*Correspondence: mzhang@ust.hk
DOI 10.1016/j.molcel.2007.10.028

SUMMARY

Multiple PDZ domain scaffold protein Par-3 and phosphoinositides (PIPs) are required for polarity in diverse cell types. We show that the second PDZ domain of Par-3 binds to phosphatidylinositol (PI) lipid membranes with high affinity. We further demonstrate that a large subset of PDZ domains in mammalian genomes are capable of binding to PI lipid membranes, indicating that lipid binding is the second most prevalent interaction mode of PDZ domains known to date. The biochemical and structural basis of Par-3 PDZ2-mediated membrane interaction is characterized in detail. The membrane binding capacity of Par-3 PDZ2 is critical for epithelial cell polarization. Interestingly, the lipid phosphatase PTEN directly binds to the third PDZ domain of Par-3. The concatenation of the PIP-binding PDZ2 and the lipid phosphatase PTEN-binding PDZ3 endows Par-3 as an ideal scaffold protein for integrating PIP signaling events during cellular polarization.

INTRODUCTION

The *par*titioning-defective (Par) proteins, originally identified in *C. elegans* and subsequently found in many other organisms, are among the first set of proteins that were identified to play critical roles in cell polarity (Kemphues, 2000; Macara, 2004; Suzuki and Ohno, 2006). Among the Par proteins, Par-3 and Par-6 form a tripartite complex with atypical protein kinase C. The complex is restricted at the anterior cortex of the zygote and is required to establish anterior/posterior polarity in *C. elegans* (Etemad-Moghadam et al., 1995; Kemphues et al., 1988; Tabuse et al., 1998). The *Drosophila* Par-3 (also called Bazooka)/Par-6/aPKC complex is also localized at the anterior cortex of eggs and is critical for the embryonic development of the animal (Benton and St Johnston, 2003; Huynh et al., 2001). In mammals, the Par-3/Par-6/aPKC complex is localized at the apical side of epithelial cells and is essential for their apical-basal polarity (Chen and Macara, 2005; Hurd et al., 2003; Plant et al., 2003; Suzuki et al., 2001). Polarization of neurons requires the Par-3/Par-6/aPKC complex as well (Nishimura et al., 2005; Shi et al., 2003; Zhang and Macara, 2006).

In addition to the common set of proteins, phosphoinositides (PIPs) are also known to play critical roles in cell polarity. Polarization and directed migration of neutrophils, macrophages, and *Dictyostelium* cells require coordinated actions of phosphatidylinositol 3-kinase (PI3K) and the antagonizing phosphatase PTEN (Funamoto et al., 2002; Iijima and Devreotes, 2002; Sasaki et al., 2004; Vanhaesebroeck et al., 1999; Wang et al., 2002). PI3K and PTEN are also required for apical-basal polarization of epithelial cells (Pinal et al., 2006; von Stein et al., 2005) and polarization of neurons (Shi et al., 2003). The Par-3/Par-6/aPKC complex is closely linked to the PIP signaling events. In neurons, Par-3 and Par-6 colocalize with active PI3K at the tip of nascent axon, and forced overexpression of PTEN leads to the failed enrichment of Par-3 at the tip of the nascent axon and compromises neuronal polarization (Shi et al., 2003). Direct interaction of Par-3 with two Rac GEFs, Tiam1 and STEF, has the potential to establish a positive feedback loop for PI3K-mediated PIP3 production important for neuronal polarization (Chen and Macara, 2005; Nishimura et al., 2005). In *Drosophila*, PTEN is recruited to zonula adherens through direct binding of PTEN to the PDZ domains of Par-3/Bazooka (Pinal et al., 2006; von Stein et al., 2005), although the biochemical basis of the PTEN/Par-3 interaction is not well characterized.

Both Par-3 and Par-6 are PDZ domain-containing scaffold proteins capable of binding to a diverse range of cell polarity regulating proteins (Macara, 2004; Suzuki and Ohno, 2006). Although best known as protein-protein interaction modules, PDZ domains were recently shown to bind to phosphatidylinositol (PI) lipids (Mortier et al., 2005; Yan et al., 2005; Zimmermann et al., 2002). The interaction between PDZ domains and PI lipids is likely to be significant, as such interactions can not only regulate membrane localization of PDZ domain proteins but also provide a potential mechanism for sensing PIP signaling by PDZ domain proteins. In contrast to a number of well-characterized lipid-binding

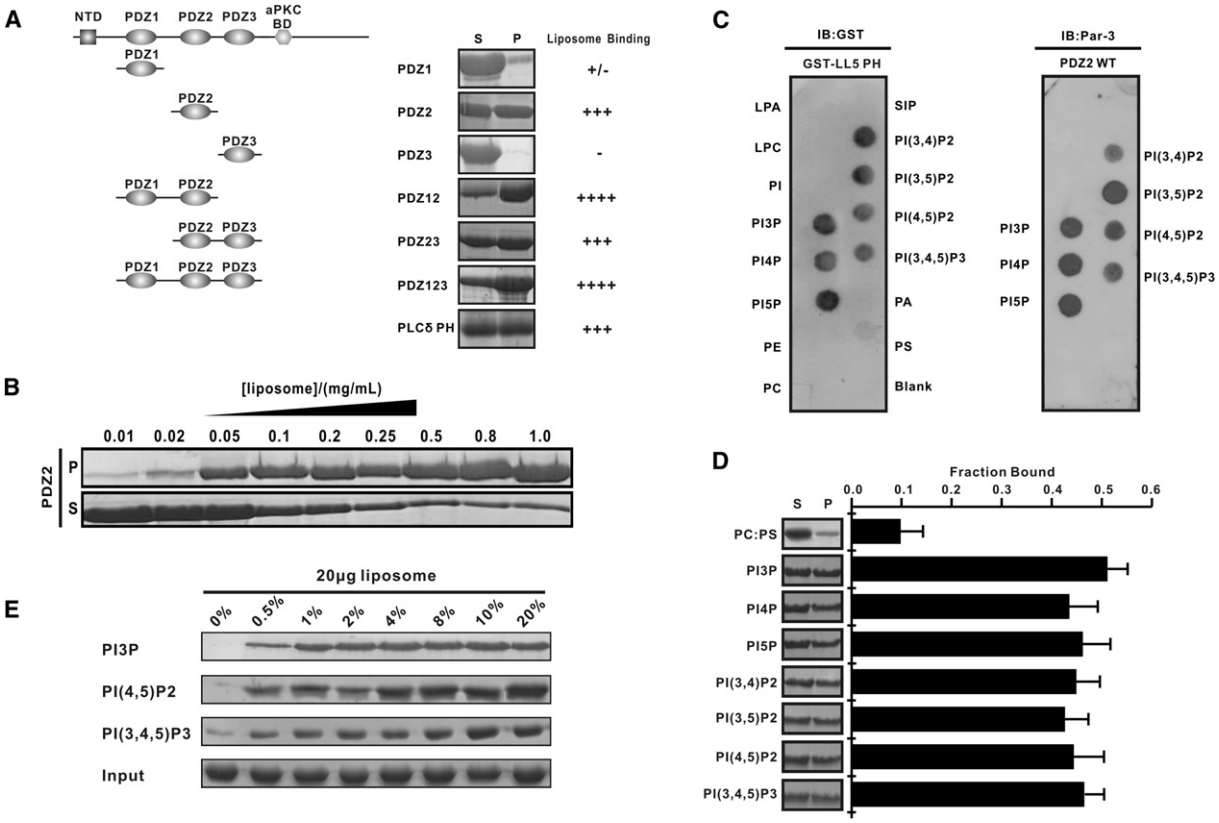

Figure 1. Binding of Par-3 PDZ2 to PIPs

(A) Lipid sedimentation assay of bindings of Par-3 PDZ domains to bovine brain liposomes. Fractions labeled with "S" and "P" represent proteins present in supernatants and pellets after centrifugation. "NTD" represents the N-terminal polymerization domain, and "aPKC-BD" stands for the aPKC binding domain of Par-3.

(B) Dose-dependent interaction of Par-3 PDZ2 with brain liposomes. In this experiment, the total amount of PDZ2 in each assay was fixed when the concentration of liposomes was increased.

(C) The lipid strip-based binding assay of Par-3 PDZ2. GST-LL5 PH (the PH domain from human LL5, supplied by Echelon) served as the positive control of the assay.

(D) Interaction of Par-3 PDZ2 with 10% various PIPs reconstituted into defined PC/PS (60%/30%) liposomes. The bar graph depicts the fraction of Par-3 PDZ2 recovered in the liposome-bound pellet in each sedimentation assay. Values are mean ± SD of three different experiments.

(E) Interaction of Par-3 PDZ2 with reconstituted PC/PS liposomes containing various concentrations of PI3P, PI(4,5)P2, and PI(3,4,5)P3, respectively. In this assay, the concentration of PC was fixed at 60%, and the concentration of PS was varied from 40% to 20% when concentration of PIPs was increased from 0% to 20%. "Input" denotes the total amount of PDZ2 used for each binding assay by Coomassie blue staining.

modules such as PH, FYVE, and PX domains, the biochemical and structural mechanisms governing the interactions between PDZ domains and PI lipids are poorly understood.

In this study, we discover that the second PDZ domain of Par-3 is capable of binding to PI lipids. We further demonstrate that binding to PIPs is a general property for a subset of PDZ domains in mammalian genomes. We show that the lipid-binding capacity of PDZ2 is critical for Par-3's function in epithelial cell polarization. Finally, we discover that the third PDZ domain of Par-3 directly binds to the lipid phosphatase PTEN. Our data suggest that the PDZ domains of Par-3 may serve as the organization center for integrating PIP signaling events in polarized cells.

RESULTS

The Second PDZ Domain of Par-3 Binds to PIPs with High Affinity

Given the paramount roles of the Par-3/Par-6/aPKC complex and PIPs in cell polarity, we tested potential direct interactions of the two Par proteins with membranes containing PI lipids. The isolated PDZ2 and any Par-3 fragments containing PDZ2 showed robust binding to liposomes prepared from total bovine brain lipid extracts (Figure 1A). In this assay, Par-3 PDZ2 and the PH domain from PLCδ displayed comparable lipid-binding affinities. The isolated PDZ3 showed no detectable binding to liposomes, and PDZ1 alone bound to liposomes very weakly. Furthermore, Par-3 PDZ2 binds to brain liposomes in

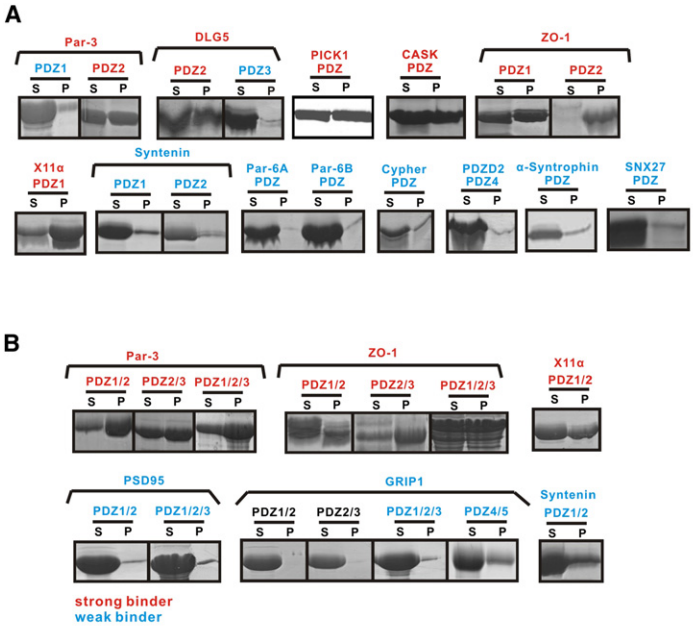

C

PDZ domains	Liposome binding affinity	PDZ domains	Liposome binding affinity
PDZ1-MUPP1	-	PDZ1-ZO1	+++
PDZ2-MUPP1	-	PDZ2-ZO1	+++
PDZ3-MUPP1	-	PDZ3-ZO1	-
PDZ4-MUPP1	-	PDZ3-MAGI3	-
PDZ5-MUPP1	-	PDZ4-MAGI3	-
PDZ6-MUPP1	-	PDZ5-MAGI3	-
PDZ7-MUPP1	-	PDZ6-MAGI3	-
PDZ8-MUPP1	-	PDZ1-Syntenin	+
PDZ9-MUPP1	-	PDZ2-Syntenin	+
GST-PDZ10-MUPP1	-	PDZ3-SAP102	-
PDZ11-MUPP1	-	PDZ-Erbin(LAP2)	-
PDZ12-MUPP1	-	PDZ1-Par3	+
PDZ13-MUPP1	-	PDZ2-Par3	+++
PDZ1-PDZRN3	-	PDZ3-Par3	-
PDZ2-PDZRN3	-	PDZ-RhoGAP21	-
PDZ1-SAP97	-	PDZ-SIPA1L2	-
PDZ2-SAP97	-	PDZ3-Harmonin	-
PDZ3-SAP97	-	PDZ-NeurabinII	-
PDZ1-DLG5	-	PDZ-GRASP	-
PDZ2-DLG5	+++	PDZ-Par6A	+
PDZ3-DLG5	+	PDZ-Par6B	+
PDZ1-X11α	+++	PDZ-CASK	+++
GB1-PDZ2-X11α	-	PDZ-PICK1	+++
PDZ1-PSD95	-	PDZ-α-Syntrophin	+
PDZ2-PSD95	-	PDZ-Myosin18	-
PDZ3-PSD95	-	PDZ-PDZK10	-
PDZ2-PDZD2	-	PDZ-HtrA4	-
PDZ4-PDZD2	+	PDZ-Mals2	-
PDZ6-PDZD2	-	PDZ3-ZO3	-
PDZ1-GRIP1	-	PDZ-Pals1	-
PDZ2-GRIP1	-	PDZ-Rim2	-
PDZ3-GRIP1	-	PDZ-nPIST	-
PDZ6-GRIP1	-	PDZ-Cypher2c	+
PDZ7-GRIP1	-	PDZ-Lop7	-
PDZ1-hSCRIB(LAP4)	-	PDZ2-NHERF2	-
PDZ2-hSCRIB(LAP4)	-	PDZ-Shank1	-
PDZ3-hSCRIB(LAP4)	-	PDZ-SNX27	+

Figure 2. Lipid Membrane Binding Assay of Selected PDZ Domains from the Human Genome

(A) A subset of isolated PDZ domains bind to liposomes prepared from bovine brain lipid extracts. The PDZ domain display strong liposome bindings are labeled in red, and the weak liposome-binding PDZ domains are indicated in blue.

(B) Liposome-binding properties of a selected set of PDZ tandems.

(C) Summary of the liposome binding assay results of the 74 isolated PDZ domains. The PDZ domains that displayed strong lipid membrane bindings are indicated with "+++," the PDZ domains that showed moderate or weak membrane bindings are denoted with "+," and the non-lipid-binding PDZ domains are labeled with "−." In preparation of PDZ proteins, an additional ten residues were added to both termini of each PDZ domain (predicted based on the structures of PDZ domains) to ensure proper domain folding. Prior to addition of liposomes, each protein sample was precentrifuged to remove any possibility of liposome-independent protein precipitation.

a dose-dependent manner (Figure 1B). The lipid-binding specificity of Par-3 PDZ2 was probed using membrane-immobilized lipid strips. Of the 15 lipids tested, Par-3 PDZ2 only recognized PIP lipids (Figure 1C), suggesting that the interaction between PDZ2 and PIPs is relatively specific. However, the stereo specificity among different PIPs is not high. To avoid potential pitfalls frequently encountered in lipid strip-based assays, we repeated assays of the binding between Par-3 PDZ2 and reconstituted defined liposomes composed of phosphatidylcholine (PC), phosphatidylserine (PS), and each PIP at a ratio of 60:30:10. The binding profiles of Par-3 PDZ2 toward various PIPs derived from the lipid strip-based assay and those from the reconstituted liposome-based assays are similar to each other (Figures 1C and 1D). We further showed that Par-3 PDZ2 binds to PIP-containing synthetic liposomes in a density-dependent manner (Figure 1E). Par-3 PDZ2 showed some basal level binding to liposomes composed of only PC and PS, and this is likely the result of nonspecific electrostatic interactions between the positively charged PDZ2 and the negative charges on the PC/PS membrane surface (see below for details). Taken together, the above data demonstrate that Par-3 PDZ2 can directly bind to PIPs and membrane bilayers containing PIPs.

PI Lipid Binding Is a General Property of a Subset of PDZ Domains

The concept that, in addition to binding to peptide ligands, PDZ domains can also function as PIP-binding modules is still in its infant stage. To test whether interaction with PIPs is a general property of PDZ domains, we assayed lipid bindings of 74 randomly selected, individual human PDZ domains and 14 PDZ tandems (Figure 2). All these PDZ proteins were purified to homogeneity. Because formation of protein aggregations will interfere with centrifugation-based lipid-binding assay, the last step of each protein purification was gel filtration chromatography and only monodispersed fractions were collected for lipid-binding assay. The number of isolated PDZ domains included in this assay represent ~1/4 of all PDZ domains in the human genome. We have also included a number of PDZ tandems in our lipid-binding assay, as tandem PDZ repeats have been shown to have distinct structural and functional features (Feng et al., 2003; Grootjans et al., 2000; Long et al., 2003, 2005). Among 74 isolated PDZ domains, 17 were found to have detectable lipid-binding capacities (Figure 2A). Among the positive binders, an additional five were found to bind to lipid membrane with affinities comparable to or even higher than Par-3 PDZ2 (e.g., ZO-1 PDZ2 or PICK1 PDZ). We noted that PDZ tandems

often bind to lipid membranes stronger than their respective isolated PDZ domains (Figure 2B). The ratio of lipid-binding PDZ domains to the total PDZ domains is similar to the ratio of lipid-binding PH domains to the total PH domains (Yu et al., 2004). We further demonstrate that PDZ domain/lipid interaction is PIP dependent (see Figure S1 available online). Taken together, we conclude that binding to PI lipid membranes is a general property of a subset of PDZ domains.

Structure and Peptide Binding Properties of Par-3 PDZ2

The strong interaction between Par-3 PDZ2 and PI lipid membrane offered us an excellent opportunity to characterize the interaction in detail. First, we determined the structure of Par-3 PDZ2 by NMR spectroscopy (Figures 3A and 3B and Table S1). Par-3 PDZ2 adopts a canonical PDZ domain fold with a classical "GLGF" motif connecting βA and βB and a regular peptide binding "αB/βB groove" (Figures 3B and 3C). The Par-3 PDZ2 structure suggests that Par-3 PDZ2 should be able to interact with peptide ligands. Indeed, several peptides were found to bind to Par-3 PDZ2 with K_D in tens of micromolar range (Figure S2A). One of the synthetic peptides with the last five residues of "LETRV" (referred to as the "LETRV peptide") binds to Par-3 PDZ2 with K_D of ~15 μM. NMR studies showed that the LETRV peptide binds to the αB/βB groove of the PDZ domain (Figures S2B and S2C).

Par-3 PDZ2 Contains a Positively Charged Surface Essential for Binding to Lipid Membranes

Amino acid sequence analysis reveals that Par-3 PDZ2 is highly abundant in positively charged residues with a theoretical isoelectric point of ~10.1 (Figure 3C). The majority of these positively charged residues are located at the one side of the domain, causing it to contain a strong positively charged surface potential (Figure 3D). We reasoned that this positively charged surface is likely to play important roles in binding to negatively charged lipid membrane surfaces. To test this hypothesis, we substituted one or more of the positively charged residues with neutral Ala or with negatively charged Glu and tested the lipid-binding capacities of these mutants. Substitutions of these positively charged residues with neutral Ala significantly decreased the lipid binding of the domain. Conversion of these positively charged residues to negatively charged Glu led to nearly complete abolishment of the lipid binding (Figures 3E and 3F). Taken together, the structural and biochemical data demonstrate that the abundant positively charged residues in Par-3 PDZ2 play critical roles in binding to the negatively charged phospholipid membrane surfaces.

Identification of the PIP Binding Site of Par-3 PDZ2

We next mapped the PIP binding site of Par-3 PDZ2 using NMR spectroscopy. Because Par-3 PDZ2 binds to mono-, bis-, and tris-PIPs with comparable affinities (Figures 1C–1E), PI3P was chosen for studying the interaction between Par-3 PDZ2 and PIPs. Titration of ^{15}N-labeled Par-3 PDZ2 with water-soluble di-C8 form of PI3P induced chemical shift changes to a specific set of residues (Figure S3), indicating direct interaction between the lipid and the PDZ domain. The interaction between PI3P and Par-3 PDZ2 was further confirmed by a transferred NOE experiment (Figure S4). We repeated the titration of Par-3 PDZ2 with other PIPs, including PI(4,5)P2 and PI(3,4,5)P3, and similar lipid-binding-induced chemical shift perturbation patterns were observed (data not shown). Mapping of the residues that experienced PI3P-induced chemical shift changes to the structure of the domain revealed that lipid binding is restricted within a defined area (Figure 4A). Specifically, the αB/βF loop and the βA/βB loop displayed the largest chemical shift changes, suggesting that these two loops are primarily responsible for binding to the PI3P head. Analysis of the Par-3 PDZ2 surface structure reveals that a polar pocket with a size suitable for accommodating the PI3P head group is formed by residues from the αB/βF and βA/βB loops (Figure 4B). Indeed, the head group of PI3P (as well as PI[4,5]P2 and PI[3,4,5]P3) can be modeled to fit snugly into this pocket. The two highly conserved and positively charged residues at the base of the pocket, Arg532 and Lys535, can interact with the phosphate group(s) from the lipid head group, and the side chain of the conserved Glu469 is positioned to form hydrogen bonds with the hydroxyl groups of the inositol ring of the lipid head (Figure 4B).

We evaluated the role of the residues in the lipid head-binding pocket by measuring the binding affinities of Par-3 PDZ2 and its mutants toward defined PC/PS vesicles containing 10% PI3P. The wild-type Par-3 PDZ2 binds to PC/PS/PI3P vesicles with an apparent dissociation constant of ~8 μM (Figure 4C). The dissociation constant of Par-3 PDZ2 toward PI3P depends on the density of PI3P embedded in PC/PS vesicles (Figure S5). Substitution of Arg532 with an Ala led to an ~11-fold decrease of binding between the PDZ domain and lipid vesicles. Mutations of Lys535 to Ala nearly abolished its lipid vesicle binding. As expected, the Arg532Lys535 to Ala double mutation completely abolished the lipid vesicle binding of Par-3 PDZ2 (Figure 4C). The existence of a negatively charged residue in the PIP head group-binding pocket is a common feature of a number of well-characterized lipid-binding domains (DiNitto et al., 2003). Consistent with this notion, mutation of Glu469 to Ala led to an ~10-fold decrease in PI3P vesicle binding of the PDZ domain (Figure 4C).

We note that the lipid head-binding pocket of Par-3 PDZ2 is situated side by side with the positive charge cluster consisting of Lys491, Lys506, Arg546, and Arg496 (Figure 4B). This spatial arrangement is ideally suited for the domain to interact with the negatively charged membrane bilayer and the PIP head groups extending from the membrane bilayer. We further note that the PIP head group-binding pocket and the positive charge cluster are separated by three hydrophobic residues (Leu494, Pro495, and Ile500), and these residues are expected to be in close vicinity of membrane bilayer and may even

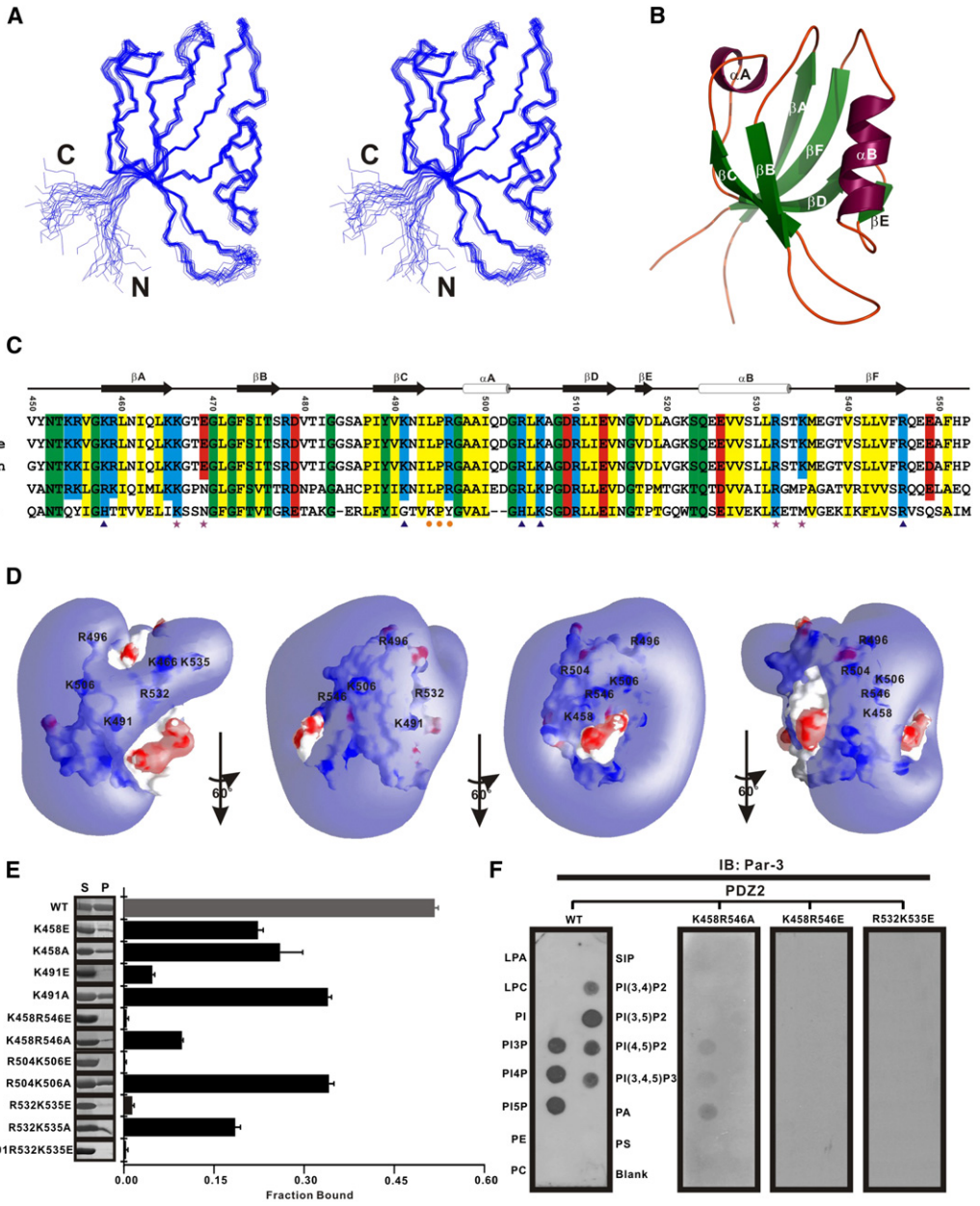

Figure 3. Structural and Biochemical Characterization of Par-3 PDZ2

(A) Stereo view showing the backbones of 20 superimposed NMR structures of Par-3 PDZ2.

(B) Ribbon diagram of a representative NMR structure of Par-3 PDZ2.

(C) Structure-based sequence alignment of Par-3 PDZ2 from different species. The residues forming the positive charge cluster important for membrane interaction are highlighted with blue triangles. The amino acids forming the PI head group binding pocket are marked with purple stars. The hydrophobic residues that may insert into the membrane bilayer are indicated with orange dots.

(D) GRASP view of the positive charge potential of Par-3 PDZ2. The residues contributing to the positive charge potential are labeled.

(E) Analysis of the roles of the positively charged residues in lipid membrane binding by sedimentation assays of the various PDZ2 mutants. Values are mean ± SD of three different experiments.

(F) Representative data from the PIP strip assay demonstrate that the positively charged residues of PDZ2 are required to bind to PIPs.

directly insert into it. We used fluorescence spectroscopy to test the above possibility. In this assay, the amino acid residues to be tested were mutated to Cys, and each mutant Par-3 PDZ2 was labeled with fluorescence probe IAEDANS. If an amino acid residue is involved in the insertion into the membrane bilayer, the attached IAEDANS undergoes fluorescence intensity enhancement upon transfer from an aqueous environment to a hydrophobic

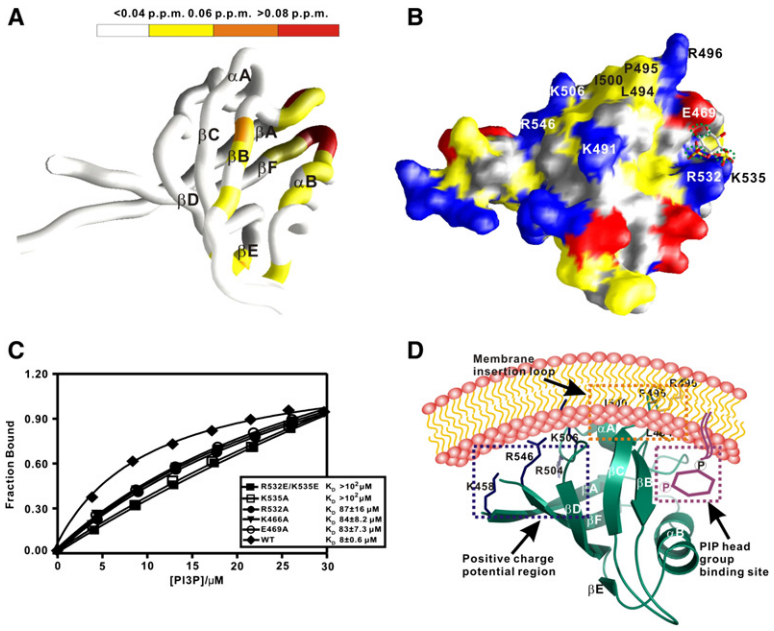

Figure 4. Mapping of the PIP Head Group Binding Site of Par-3 PDZ2

(A) The worm model showing a summary of the chemical shift changes of Par-3 PDZ2 induced by the binding of di-C_8 PI3P. The scale of the changes is shown at the top.

(B) A structure model of Par-3 PDZ2 in complex with the head group of PI3P. Par-3 PDZ2 is in surface representation. Positive residues are drawn in blue, negative residues in red, hydrophobic residues in yellow, and all the others in white. The PIP head group is shown with explicit atom representation.

(C) Fluorescence-based assay compares the apparent K_D values of the wild-type Par-3 and its mutants in binding to reconstituted PC/PS (60%/30%) containing 10% PI3P.

(D) A schematic model summarizing the interaction of Par-3 PDZ2 with PI lipid membranes. In this model, the positive charge cluster (highlighted with blue box) is in direct contact with the negatively charged membrane surface and the PIP head group binding pocket (shown in purple box) is juxtaposed with the positive charge cluster to the membrane bilayer. The hydrophobic residues (in orange box) located between the positive charge cluster and the lipid head-binding pocket insert into the membrane bilayer.

milieu (Crowley et al., 1993). Indeed, both the Pro495Cys and Leu494Cys mutants of Par-3 PDZ2 underwent substantial fluorescence intensity increases upon binding to PC/PS/PI3P vesicles, and the observed fluorescence intensity increases are specific to the existence of PI3P in the vesicles (Figures 5A and 5B, and the location of the residues in Figure 5G). As controls, when the IAEDANS probe was placed at the positions of Met536 (a hydrophobic residue at the opposite side of the proposed membrane-binding surface of the domain) or the very C-terminal end of Par-3 PDZ2, no fluorescence intensity increases were observed (Figures 5D and 5E). The Arg496Cys mutant of Par-3 PDZ2 showed substantial fluorescence intensity increase upon the binding of the domain to the lipid vesicles (Figure 5C). Arg496 is immediately above the PIP head group binding pocket, and this residue is expected to be in close vicinity to the membrane bilayer (Figure 5G). The fluorescence intensity of Lys506 mutant is partially increased, as this site is expected to be near the membrane bilayer (Figures 5F and 5G). Figure 5H summarizes the residues on Par-3 PDZ2 that were investigated by the IAEDANS probe. The fluorescence enhancement data fit well with the lipid-binding data shown in Figures 3 and 4. Summarizing all structural and biochemical data above, a model is constructed to describe the interaction of Par-3 PDZ2 with PIP-containing lipid membrane bilayers (Figure 4D). Finally, we noted that the PIP head group-binding pocket of Par-3 PDZ2 partially overlaps with the peptide ligand binding site of the domain (Figure 4A and Figure S2). We demonstrated that peptide ligand binding and PIP binding are mutually exclusive (Figures S6A and S6B).

The PIP Phosphatase PTEN Binds to Par-3 PDZ3

A recent study suggested that both PDZ2 and PDZ3 of Par-3 are required for its direct interaction to PTEN (von Stein et al., 2005), although it is difficult to conceptualize why both PDZ domains are required to bind to the single carboxyl tail of PTEN. To resolve this issue, we studied the interaction between PTEN and Par-3 in detail. When overexpressed in HEK293T cells, the full-length PTEN and Par-3 can interact with each other (Figure 6A). We further demonstrate that the two proteins interact with each other at their endogenous levels in MDCK II cells (Figure 6B). Using a purified GST-PTEN peptide, we demonstrated that the carboxyl tail of PTEN binds to PDZ2/3 and PDZ3 but not to PDZ2 of Par-3 (Figures 6C and 6D). As expected, the interaction between Par-3 PDZ3 with PTEN requires the carboxyl tail of PTEN, as deletion of the last ten amino acid residues completely abolished PTEN's binding to Par-3 PDZ3 (Figure 6E). Using a fluorescence-labeled PTEN peptide, we measured the binding affinities of PTEN toward various combinations of Par-3 PDZ domains (Figure 6F). Consistent with the data shown in Figures 6A–6D, Par-3 PDZ3 binds to the PTEN peptide with a significantly higher affinity than the PDZ2 domain. In an NMR-based titration experiment, we could not detect any binding between Par-3 PDZ1 and the PTEN peptide (data not shown).

The Membrane Binding of PDZ2 Is Important for Par-3-Mediated Epithelial Cell Polarization

We next tested physiological relevance of the Par-3 PDZ2-lipid interaction observed in this study. First, we assessed the role of the PI lipid binding of Par-3 PDZ2 in

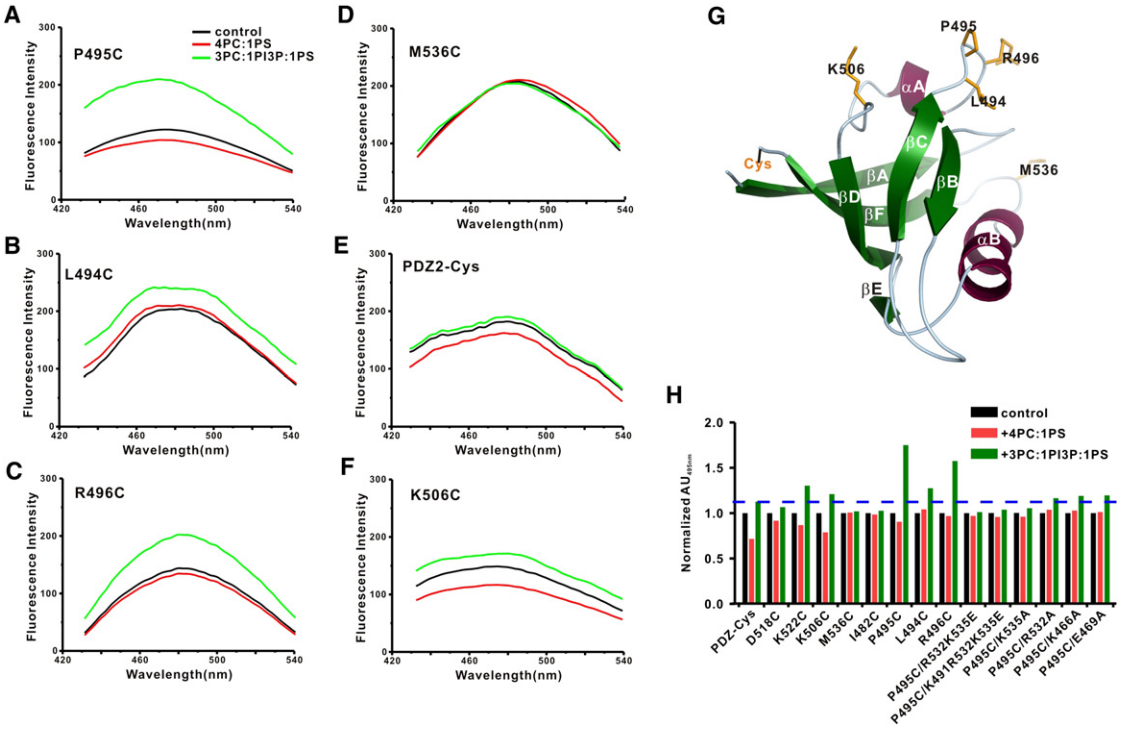

Figure 5. Identification of the Membrane Bilayer Insertion Site of Par-3 PDZ2

(A–F) IAEDANS fluorescence spectra of Par-3 PDZ2 with the probe positioned at the indicated residues. Three fluorescence spectra (protein in buffer, protein with PC/PS vesicles, and the protein with the PC/PS/PI3P vesicles) were recorded for each sample.

(G) Ribbon diagram of Par-3 PDZ2 showing the positions of the fluorescence probe.

(H) Summary of the IAEDANS-based fluorescence assays of all Par-3 PDZ2 mutants. The black, red, and blue bars represent the fluorescence intensity at 495 nm of each protein in the absence of vesicles, in the presence of 5 μM PC/PS vesicles, and in the presence of 5 μM PC/PS/PI3P vesicles, respectively. The blue line is to indicate the mutants showing significant PI3P-induced fluorescence intensity enhancements.

the protein's membrane localization in MDCK cells. As expected, the majority of the wild-type Par-3 is localized to cell membrane (Figures 7A and 7B). Deletion of PDZ2 ("ΔPDZ2") led to a nearly complete loss of membrane localization of the mutant Par-3, indicating that PDZ2 plays a critical role in the membrane localization of Par-3. We constructed two double mutants (K458R546E and R504K506E) and a quadruple mutant (K458R546R 504K506E, denoted as "K4E") of Par-3. Mutations of these positive residues essentially abolished the lipid binding of the PDZ domain but had very little impact on the peptide ligand binding of the PDZ domain (Figure 3E and data not shown). The large decreases of membrane localization of these three Par-3 mutants indicate that the PI lipid binding, not the peptide ligand binding, is required for Par-3 to localize to membranes (Figure 7A). Substitutions of Arg532, Lys535, and Lys491 with Glu led to decreases in lipid binding of Par-3 PDZ2 (Figure 3E). As expected, the R532K535E double mutant and the K491R532K535E triple mutant ("K3E") of Par-3 displayed decreased membrane localization. We used both gain- and loss-of-function chimeras of Par-3 to confirm that the PI lipid binding of Par-3 PDZ2 is important for the protein's localization to membranes in MDCK cells. The PDZ domain of Mals2/mLin-7b and Par-3 PDZ2 display similar peptide binding properties (the dissociation constant of the Mals2 PDZ/the LETRV peptide is ~10 μM; H.W. and M.Z., unpublished data), but the Mals2 PDZ shows no detectable lipid binding (Figure 2C). The Par-3 chimera with its PDZ2 replaced with the PDZ domain of Mals2 ("Mals2 PDZ") was defective in membrane localization (Figure 7A). In a complementary experiment, we replaced Par-3 PDZ2 with the PH domain of PLCδ, which is known to bind to PI(4,5)P2 with high affinity. The chimera Par-3 ("PLCδ PH") localized to membrane as well as or even better than the wild-type Par-3 (Figure 7A). The histogram in Figure 7B is a summary of each Par-3 mutant's localization in MDCK cells.

Because localization to the tight junction membrane in polarized MDCK cells is a hallmark for Par-3, we predict that Par-3 mutants defective in membrane localization would also be defective in the Par-3-mediated polarization of MDCK cells. To test this hypothesis, we measured the abilities of the wild-type rat Par-3 and its mutants in rescuing MDCK cells' repolarization after "calcium switch." In normal calcium-containing medium (HCM), overexpression of the wild-type or various mutants of Par-3 have limited effects on the tight junction formation in MDCK

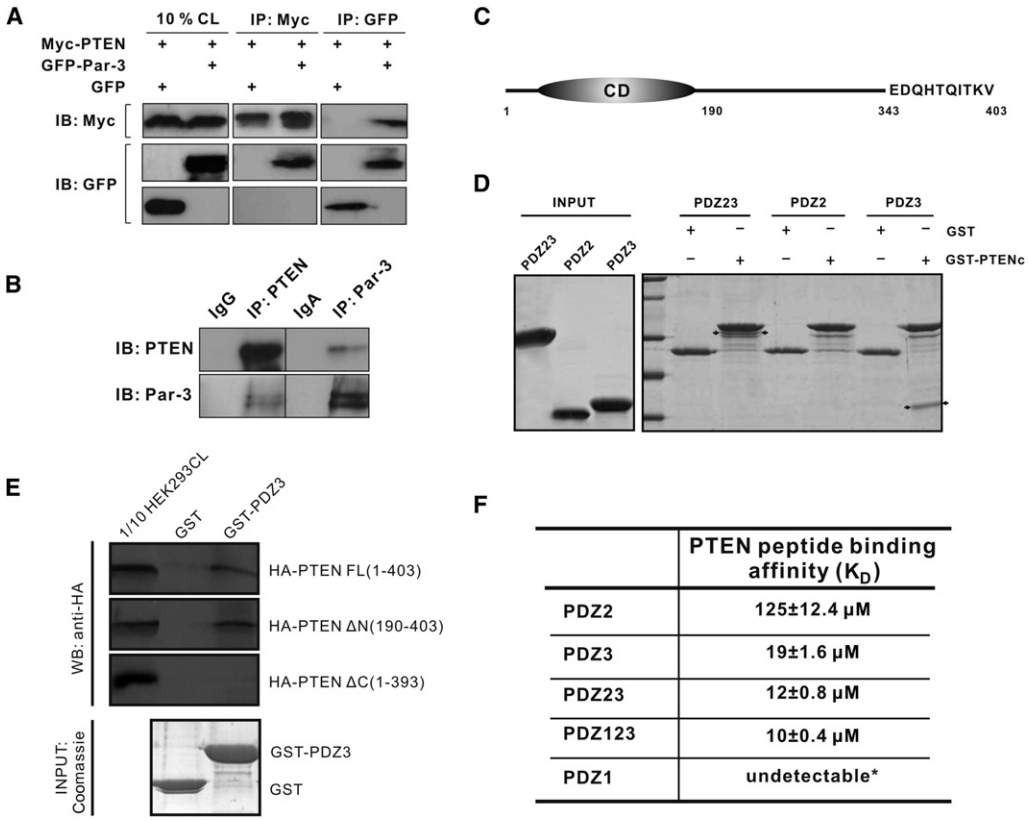

	PTEN peptide binding affinity (K_D)
PDZ2	125±12.4 μM
PDZ3	19±1.6 μM
PDZ23	12±0.8 μM
PDZ123	10±0.4 μM
PDZ1	undetectable*

Figure 6. The Lipid Phosphatase PTEN Binds to Par-3 PDZ3

(A) Overexpressed Par-3 and PTEN associated with each other. The figure shows that Myc-tagged PTEN and GFP-tagged Par-3, when coexpressed in HEK293T cells, interact with each other in reciprocal coimmunoprecipitation assays. GFP was used as the control for the interaction specificity. The loading control is 10% of total cell lysate (CL).

(B) Coimmunoprecipitation assay demonstrates that the endogenous levels of Par-3 and PTEN interact with each other in MDCK II cells.

(C) Domain organization of rat PTEN. PTEN contains a catalytic domain (CD) and a C-terminal PDZ-binding motif.

(D) Coomassie blue staining showing that GST-fused PTEN peptide (GST-"EDQHTQITKV") robustly binds to PDZ23 and PDZ3 (bands indicated by arrows), but not to PDZ2 of Par-3. The amount of PDZ proteins used in the assay is indicated as "INPUT" at the left.

(E) Pull-down experiment showing that the carboxyl tail of PTEN is required for binding to Par-3 PDZ3. In this experiment, purified GST-PDZ3 was used to pull down HA-tagged PTEN expressed in HEK293T cells. The amount of GST-PDZ3 and the GST control used in the binding assay are shown in Coomassie blue staining at the bottom.

(F) The binding affinities of the FITC-labeled PTEN peptide to the Par-3 PDZ domains measured by fluorescence polarization-based binding assay.

cells (Hirose et al., 2002; Chen and Macara, 2005; and Figure 7D). In agreement with an earlier study (Chen and Macara, 2005), knockdown of the endogenous canine Par-3 by RNA interference (RNAi) caused a dramatic disruption of tight junction assembly after calcium switch, and this tight junction assembly defect can be rescued by cotransfection of the wild-type, RNAi-resistant rat Par-3 (Figures 7C–7E). Supporting our prediction, the two Par-3 mutants, one with the entire PDZ2 deleted (ΔPDZ2) and the other with three positively charged residues mutated to Glu (K3E, also see Figure 7A), were not able to rescue epithelial cell repolarization after the knockdown of the endogenous Par-3. We further demonstrate that the Par-3 chimera with its PDZ2 replaced by PLCδ PH was also capable of rescuing the polarization of MDCK cells caused by the loss of the endogenous Par-3 (Figures 7D and 7E). Taken together, the data shown in Figure 7 strongly support our conclusion that the PDZ2-PI lipid membrane binding is critical for Par-3 in regulating epithelial cell polarization.

DISCUSSION

PDZ domains are best known for their ability to bind to peptide ligands situated at the extreme carboxyl tail of target proteins. In this work, we demonstrated that a significant number of PDZ domains in the human genome are also capable of binding to PIP-containing lipid membranes. To elucidate the molecular basis governing PDZ/PI lipid interactions, we characterized the binding of Par-3 PDZ2 to PI lipid membranes in detail. The 3D structure of Par-3 PDZ2 revealed that the domain contains a flat surface rich in positively charged residues, and this positively charged surface is juxtaposed with the peptide ligand

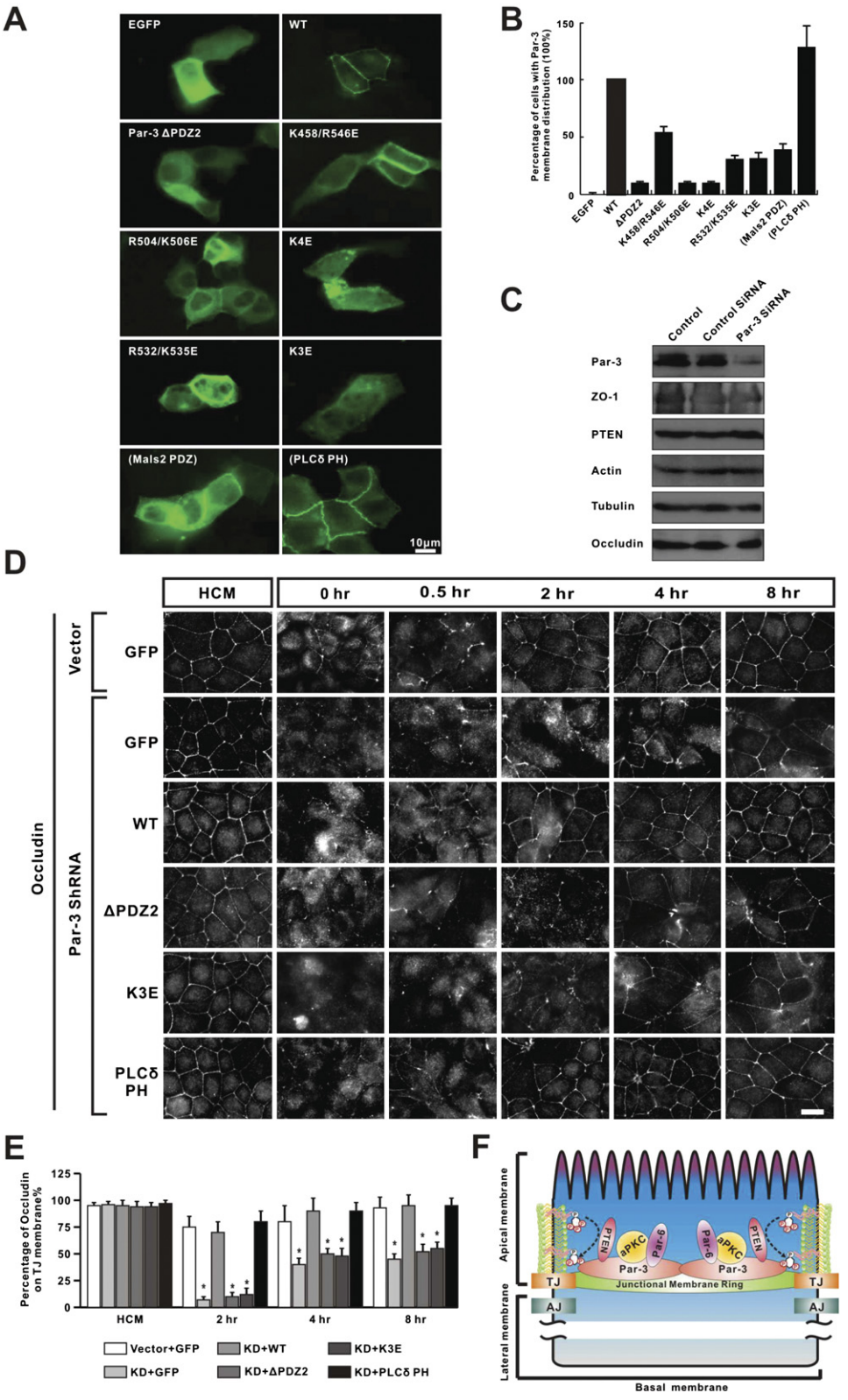

Figure 7. The Par-3 PDZ2-Lipid Membrane Interaction Is Critical for Epithelial Cell Polarization

(A) Comparison of the membrane localization changes of various Par-3 mutants and chimeras. As the control, EGFP is diffusely localized throughout the cells.

binding groove of the PDZ domain (Figures 3 and 4). Par-3 PDZ2 contains a surface with large positive charge potential, a characteristic feature also found in the majority of known PIP-binding PH domains (Lemmon and Ferguson, 2000; DiNitto et al., 2003; Yu et al., 2004). Site-directed mutagenesis studies showed that the positively charged residues on this flat surface are critical for the PDZ domain to bind to PI lipid membrane. We note with great interest that several lipid membrane-binding PDZ domains shown in Figure 2 (e.g., PDZ1 of X11α, the PDZ domain of CASK, and PDZ2 of DLG5) also contain large amounts of net positive charges. More importantly, amino acid sequence analysis revealed that the positively charged residues in Par-3 PDZ2 identified to play critical roles in binding to PI lipid membranes also exist in the corresponding positions in these PDZ domains (Figure S7). We propose that the mechanism governing the Par-3 PDZ2-lipid interaction observed in the current study can be extended to at least a subset of lipid-binding PDZ domains.

In addition to this positively charged surface, Par-3 PDZ2 contains another critical membrane interaction region located at the αB/βF loop and βA/βB loop of the domain. This region of the PDZ domain directly interacts with the head groups of PIPs. Par-3 PDZ2 displays little specificity toward different PIPs. It was shown that the PDZ domain of α-syntrophin also showed no specificity toward various PIPs (Yan et al., 2005). Additionally, we found that the PDZ domains that we have tested showed little specificity toward PIPs. We predict that, analogous to PH domains (Yu et al., 2004), the majority of PIP-binding PDZ domains have little lipid-binding specificity. However, we cannot rule out that some PDZ domains in the mammalian genomes may bind to lipids specifically, as we have only covered about a quarter of PDZ domains in the current study.

The simultaneous binding of PIPs and their antagonizing phosphatase PTEN to Par-3 is particularly interesting in the context of cell polarity control. Increasing evidence indicates that Par-3 often segregates from the obligatory Par-6/aPKC complex in various cell types (Chen and Macara, 2005; Etienne-Manneville and Hall, 2001; Harris and Peifer, 2005; Nam and Choi, 2003; Tabuse et al., 1998). The active PI3K signal and the production of PI(3,4,5)P3 lead to the activation of both aPKC and Par-6. We demonstrated that the PDZ2 domain-mediated membrane binding is critical for proper membrane localization of Par-3 in MDCK cells (see a model in Figure 7F). The positioning and the multimodular property of Par-3 make it ideally suited to be a physical barrier in preventing possible "leakages" of PI(3,4,5)P3 from the apical domain to the basal-lateral domain in polarized epithelial cells. The PIP-binding PDZ2 domain is connected to the PTEN-binding PDZ3 domain with a linker of ~25 residues. Such PDZ domain organization should ensure that PI(3,4,5)P3 crossing the tight junction membrane ring is trapped by Par-3 PDZ2 and quickly hydrolyzed by PTEN juxtaposed with the PDZ2/lipid complex via the PDZ3 domain. The N-terminal domain-mediated Par-3 oligomerization (Feng et al., 2007) further enhances the capacity of Par-3 in capturing PIPs as well as in anchoring PTEN. Therefore, the Par-3/PTEN complex at the tight junction membrane ring may function as an "insulator" for compartmentalized distribution of PIPs in polarized cells. Although speculative, our hypothesis serves as a framework for further experiments to test the roles of Par-3 in regulating concentration gradient of PIP lipids.

In summary, we discovered that the second PDZ domain of Par-3 binds to PI lipid membranes with high affinity. This Par-3 PDZ2-lipid interaction is critical for epithelial cell polarization. The strong binding between Par-3 PDZ2 and lipid membrane is conferred by an exposed positive charge cluster and a PIP head group binding pocket on the PDZ domain. We further demonstrated that binding to PIPs is a general property for a subset of PDZ domains.

EXPERIMENTAL PROCEDURES

Preparation of Proteins

The coding sequences of the individual PDZ domains and PDZ tandems of Par-3, including PDZ1 (residues 228–410), PDZ2 (454–554), PDZ3 (579–704), PDZ1/2 (228–554), PDZ2/3 (454–704), and PDZ1/2/3 (228–704), were PCR amplified from rat *Par-3* and cloned into a pET32a vector. Proteins were expressed in BL21(DE3) *Escherichia coli* cells. The His_6-tagged PDZ domains were purified using Ni^{2+}-nitrilotriacetic acid agarose column followed by size-exclusion

(B) Quantitative comparison of the levels of plasma membrane localization of various Par-3 proteins shown in (A). At least 100 individual cells were counted for each form of Par-3. Values are mean ± SD of three different experiments.

(C) Specific knockdown of endogenous canine Par-3 with RNAi. MDCK II cells were transiently transfected with empty pSUPER vector (control), pSUPER vector containing control shRNA ("Control SiRNA"), and pSUPER-shRNA specifically targeting canine Par-3 mRNA ("Par-3 SiRNA"), respectively. The data show that Par-3 knockdown did not alter the levels of the tight junction proteins ZO-1 and occludin. The level of PTEN was not affected by the Par-3 knockdown either. Actin and tubulin were used as the loading controls.

(D) Knockdown of endogenous Par-3 severely compromised repolarization of MDCK cells during a calcium switch assay. The repolarization of MDCK cells after calcium switch was assayed by staining the tight junction marker occludin. GFP was coexpressed as a marker for transfection efficiency. The scale bar stands for 10 μm.

(E) Quantification of the percentage of occludin localization at junctional membranes after calcium switch at the indicated time points. Values are mean ± SD of three randomly selected fields from imaging slides. Asterisk denotes significant difference from the Par-3 knockdown cells ($p < 0.05$ by Student's t test).

(F) A schematic model showing PDZ domain-mediated lipid membrane interaction in the localization of the Par-3/PTEN complex at the tight junction (TJ) membrane ring. The model also illustrates that Par-3 may act as a PIP signaling integrator in polarized epithelial cells. The positioning of Par-3 slightly below TJ and polymerization of Par-3 makes it ideally suited as a physical barrier in preventing possible "leakages" of PI(3,4,5)P3 from the apical domain to the basal-lateral domain in polarized epithelia.

chromatography. For in vitro biochemical analysis, the wild-type PDZ2 and its mutants were expressed as GST fusion proteins and purified using GSH-Sepharose affinity chromatography.

NMR Spectroscopy

The NMR samples were concentrated to ~0.1 mM for titration experiments and ~1.5 mM for structural determinations in 100 mM potassium phosphate at pH 6.5. NMR spectra were acquired at 30°C on Varian Inova 500 or 750 MHz spectrometers. Chemical shift assignments of Par-3 PDZ2 were achieved by combination of standard NMR experiments using $^{15}N/^{13}C$-labeled and unlabeled samples (Cavanagh et al., 1996). Approximate interproton distance restraints were derived from 2D ^{1}H-, 3D ^{15}N-, and ^{13}C-separated NOESY spectra. Structures were calculated using the program CNS (Brunger et al., 1998).

Fluorescence Assays

Fluorescence assays were performed on a Perkin Elmer LS-55 fluorimeter equipped with an automated polarizer at 20°C. For lipid vesicle binding assays, each purified Par-3 PDZ2 mutant was conjugated with a fluorescent naphthalene derivative, 5-((((2-iodoacetyl)amino)-ethyl)amino)naphthalene-1-sulfonic acid (1,5-IAEDANS, Molecular Probes), to a single Cys of each protein. Fluorescence titration was performed by adding increasing amounts of reconstituted liposomes to a fixed amount of IAEDANS-labeled Par-3 PDZ2 (~1 μM) in 40 mM HEPES buffer (pH 7.4) containing 100 mM NaCl, 1 mM EDTA, and 1 mM DTT. For fluorescence polarization assays, fluorescein-5-isothiocynate (FITC, Molecular Probes)-labeled peptide or protein samples (~1 μM) were titrated with binding partners in the same HEPES buffer, and the K_D values were obtained by fitting the titration curves with the classical one-site binding model.

Lipid-Binding Assays

Bindings of PDZ proteins to liposomes prepared from the total bovine brain lipid extracts (Folch fraction I, Sigma B1502) and PIP lipids immobilized on membrane strips (Echelon Biosciences, P-6001) were assayed as described (Yan et al., 2005).

Defined liposomes were reconstituted from synthetic PC and PS (Avanti Polar Lipids) with or without certain concentrations of PIPs (Echelon Biosciences). Lipids dissolved in chloroform were mixed in a glass tube at an appropriate ratio, and the solvent was evaporated under a stream of N_2 gas at 4°C. An appropriate amount of buffer (20 mM HEPES [pH 7.4] containing 100 mM NaCl) was added to bring the final lipid concentration to 2–10 mg/ml. The lipid solution was rigorously vortexed for 5 min, and then the mixture was hydrated by ten cycles of freeze and thaw with liquid N_2. For fluorescence titration assays, the lipid solution was then passed through a miniextruder (Avanti Polar Lipids) with a filter with pore diameter of 0.1 μM for more than ten times to form lipid vesicles with homogenous sizes.

RNAi and Par-3 Knockdown

The sequences of oligonucleotides used to knock down canine Par-3 are exactly the same as the Par-3 #3 oligonucleotide set described in an earlier study (Chen and Macara, 2005). Specifically, the Par-3 shRNA sense primer is 5′-GATCCCCAGGATAAAGCTGGCAAAG A*TTCAAGAGA*ATCTTTGCCAGCTTTATCCTTTTTTGGAAA-3′; the antisense primer is 5′-AGCTTTTCCAAAAAAGGATAAAGCTGGCAAAGA *TCTCTTGAA*ATCTTTGCCAGCTTTATCCTGGG-3′. Italics indicate the 9 bp hairpin loop. Annealed double-strand oligonucleotides were inserted into the BglII and HindIII cloning sites of the pSUPER vector.

The following primary antibodies were used in western blot to assay the knockdown efficiency of the Par-3 RNAi: polyclonal anti-Par-3 (1:1000) (Upstate), polyclonal anti-PTEN (1:1,000) (Cell Signaling); monoclonal anti-ZO-1 (1:1000) (from Dr. B. Peng), monoclonal anti-occludin (1:1000) (Zymed); and monoclonal anti-β-tubulin (1:1000) and monoclonal anti-α-actin (1:1000) (from Dr. R. Qi). HRP-conjugated donkey anti-mouse (Jackson Laboratories) or donkey anti-rabbit secondary antibodies (Cell Signaling) were used at 1:10,000 dilutions.

In Vitro and Coimmunoprecipitation Binding Assays

For GST pull-down assay, GST or GST-tagged proteins (50 μl from 1 mg/ml stock solutions) were first loaded to 20 μl of GSH Sepharose 4B slurry beads in an assay buffer (50 mM Tris-HCl [pH 7.5], 100 mM NaCl, 1 mM DTT, and 0.5% NP-40). The GST fusion protein loaded beads were then mixed with potential binding partners, and the mixtures were incubated for 2 hr at 4°C. After three times washing, the proteins captured by affinity beads were eluted by boiling, resolved by 15% SDS-PAGE, and detected either by Coomassie blue staining or by immunoblotting with specific antibodies.

For coimmunoprecipitation assays, cultured HEK293T cells transiently transfected with GFP-Par-3 and Myc-PTEN were lysed using the RIPA buffer (50 mM Tris-HCl [pH 7.4], 150 mM NaCl, 1% NP-40, 1% NaDC, 1 mM EDTA, and 1 mM PMSF). After the proteins were extracted, PTEN was precipitated with anti-Myc monoclonal antibody. The precipitants were washed and subsequently blotted with anti-GFP polyclonal antibody (Invitrogen) for the detection of the PTEN-bound Par-3. In a reciprocal experiment, Par-3 was precipitated with anti-GFP antibody, and the bound PTEN was detected with anti-Myc antibody. To immunoprecipitate the endogenous Par-3/PTEN complex from MDCK cells, Par-3 was precipitated with a polyclonal anti-Par-3 antibody by incubating the antibody with the MDCK cell lysates for 4 hr at 4°C. After washing, the precipitant was blotted with a polyclonal anti-PTEN antibody. In a reciprocal experiment, PTEN was precipitated with the anti-PTEN antibody, and the precipitant was blotted with an anti-Par-3 antibody.

Cellular Localization and Calcium Switch Assay

The wild-type Par-3 was cloned into the pEGFP-C2 vector. EGFP-Par-3 ΔPDZ2 and various EGFP-Par-3 mutants were created using the standard PCR-based method. The EGFP-Par-3 chimeras, EGFP-Par-3(Mals2 PDZ) and EGFP-Par-3(PLCδ PH), were constructed by substituting PDZ2 with the rat Mals2 PDZ (residues 94–174) and the PH domain of human PLCδ (residues 22–132), respectively. MDCK II cells were transiently transfected with 0.7 μg plasmids per well using lipofectamine *PLUS* kit (Invitrogen) and cultured for 48 hr before fixation.

Calcium switch experiments were performed as described previously (Chen and Macara, 2005). pSUPER Par-3 shRNA was delivered using nucleotransfection kit (Amaxa) into cultured MDCK II cells along with the wild-type rat Par-3 or its mutants. After electroporation, 7.5×10^5 MDCK II cells were plated in 24-well tissue culture plate with minimum essential medium (MEM from Invitrogen) containing 1.8 mM calcium (normal calcium medium, HCM), and cultured for ~40 hr. Cells were washed twice with phosphate-buffered saline (PBS) and incubated in MEM supplemented with 2% fetal bovine serum that was dialyzed in 150 mM NaCl overnight (low calcium medium, LCM). After 16 hr incubation in LCM, cells were switched back to HCM. To detect occludin and GFP, cells were washed and then fixed in 4% paraformaldehyde (PFA) for 15 min at room temperature and permeabilized with 0.2% Triton X-100 in PBS. After washing with PBS, cells were blocked with 10% normal donkey serum in PBS for 1 hr and incubated with primary (anti-occludin) and rhodamine red X-conjugated secondary antibody (anti-rabbit, Jackson's Laboratory). The images were acquired and analyzed using a Nikon TE2000E inverted fluorescent microscope.

Illustrations

The figures were prepared using MOLMOL (Koradi et al., 1996), MOLSCRIPT (www.avatar.se/molscript/), PyMOL (http://pymol.sourceforge.net/), and GRASP (Nicholls, 1992).

Supplemental Data

Supplemental Data include seven figures and one table and can be found with this article online at http://www.molecule.org/cgi/content/full/28/5/886/DC1/.

ACKNOWLEDGMENTS

We are extremely grateful to Drs. Xinyu Chen and Ian Macara for their continuous advice in the calcium switch and MDCK polarity assay experiments. We also thank Dr. Daiwen Yang for suggestions, and Mr. Anthony Zhang for editing of the manuscript. This work was supported by grants from the RGC of Hong Kong to M.Z. (HKUST6125/04M, 6419/05M, 6442/06M, and AoE/B-15/01-II). The NMR spectrometer used in this work was purchased with funds donated to us by the Hong Kong Jockey Club. M.Z. was a recipient of the Croucher Foundation Senior Research Fellow Award.

Received: April 30, 2007
Revised: July 23, 2007
Accepted: October 11, 2007
Published: December 13, 2007

REFERENCES

Benton, R., and St Johnston, D. (2003). Drosophila PAR-1 and 14-3-3 inhibit Bazooka/PAR-3 to establish complementary cortical domains in polarized cells. Cell *115*, 691–704.

Brunger, A.T., Adams, P.D., Clore, G.M., DeLano, W.L., Gros, P., Grosse-Kunstleve, R.W., Jiang, J.S., Kuszewski, J., Nilges, M., Pannu, N.S., et al. (1998). Crystallography & NMR system: a new software suite for macromolecular structure determination. Acta Crystallogr. D Biol. Crystallogr. *54*, 905–921.

Cavanagh, J., Fairbrother, W.J., Palmer, A.G., III, and Skelton, N.J. (1996). Protein NMR Spectroscopy: Principles and Practice (San Diego: Academic Press).

Chen, X., and Macara, I.G. (2005). Par-3 controls tight junction assembly through the Rac exchange factor Tiam1. Nat. Cell Biol. *7*, 262–269.

Crowley, K.S., Reinhart, G.D., and Johnson, A.E. (1993). The signal sequence moves through a ribosomal tunnel into a noncytoplasmic aqueous environment at the ER membrane early in translocation. Cell *73*, 1101–1115.

DiNitto, J.P., Cronin, T.C., and Lambright, D.G. (2003). Membrane recognition and targeting by lipid-binding domains. Sci. STKE *2003*, re16.

Etemad-Moghadam, B., Guo, S., and Kemphues, K.J. (1995). Asymmetrically distributed PAR-3 protein contributes to cell polarity and spindle alignment in early C. elegans embryos. Cell *83*, 743–752.

Etienne-Manneville, S., and Hall, A. (2001). Integrin-mediated activation of Cdc42 controls cell polarity in migrating astrocytes through PKCzeta. Cell *106*, 489–498.

Feng, W., Shi, Y., Li, M., and Zhang, M. (2003). Tandem PDZ repeats in glutamate receptor-interacting proteins have a novel mode of PDZ domain-mediated target binding. Nat. Struct. Biol. *10*, 972–978.

Feng, W., Wu, H., Chan, L.N., and Zhang, M. (2007). The Par-3 NTD adopts a PB1-like structure required for Par-3 oligomerization and membrane localization. EMBO J. *26*, 2786–2796.

Funamoto, S., Meili, R., Lee, S., Parry, L., and Firtel, R.A. (2002). Spatial and temporal regulation of 3-phosphoinositides by PI 3-kinase and PTEN mediates chemotaxis. Cell *109*, 611–623.

Grootjans, J.J., Reekmans, G., Ceulemans, H., and David, G. (2000). Syntenin-syndecan binding requires syndecan-synteny and the co-operation of both PDZ domains of syntenin. J. Biol. Chem. *275*, 19933–19941.

Harris, T.J., and Peifer, M. (2005). The positioning and segregation of apical cues during epithelial polarity establishment in Drosophila. J. Cell Biol. *170*, 813–823.

Hirose, T., Izumi, Y., Nagashima, Y., Tamai-Nagai, Y., Kurihara, H., Sakai, T., Suzuki, Y., Yamanaka, T., Suzuki, A., Mizuno, K., and Ohno, S. (2002). Involvement of ASIP/PAR-3 in the promotion of epithelial tight junction formation. J. Cell Sci. *115*, 2485–2495.

Hurd, T.W., Gao, L., Roh, M.H., Macara, I.G., and Margolis, B. (2003). Direct interaction of two polarity complexes implicated in epithelial tight junction assembly. Nat. Cell Biol. *5*, 137–142.

Huynh, J.R., Petronczki, M., Knoblich, J.A., and St Johnston, D. (2001). Bazooka and PAR-6 are required with PAR-1 for the maintenance of oocyte fate in Drosophila. Curr. Biol. *11*, 901–906.

Iijima, M., and Devreotes, P. (2002). Tumor suppressor PTEN mediates sensing of chemoattractant gradients. Cell *109*, 599–610.

Kemphues, K. (2000). PARsing embryonic polarity. Cell *101*, 345–348.

Kemphues, K.J., Priess, J.R., Morton, D.G., and Cheng, N.S. (1988). Identification of genes required for cytoplasmic localization in early C. elegans embryos. Cell *52*, 311–320.

Koradi, R., Billeter, M., and Wuthrich, K. (1996). MOLMOL: a program for display and analysis of macromolecular structures. J. Mol. Graph. *14*, 51–55.

Lemmon, M.A., and Ferguson, K.M. (2000). Signal-dependent membrane targeting by pleckstrin homology (PH) domains. Biochem. J. *350*, 1–18.

Long, J.F., Tochio, H., Wang, P., Fan, J.S., Sala, C., Niethammer, M., Sheng, M., and Zhang, M. (2003). Supramodular structure and synergistic target binding of the N-terminal tandem PDZ domains of PSD-95. J. Mol. Biol. *327*, 203–214.

Long, J.F., Feng, W., Wang, R., Chan, L.N., Ip, F.C., Xia, J., Ip, N.Y., and Zhang, M. (2005). Autoinhibition of X11/Mint scaffold proteins revealed by the closed conformation of the PDZ tandem. Nat. Struct. Mol. Biol. *12*, 722–728.

Macara, I.G. (2004). Par proteins: partners in polarization. Curr. Biol. *14*, R160–R162.

Mortier, E., Wuytens, G., Leenaerts, I., Hannes, F., Heung, M.Y., Degeest, G., David, G., and Zimmermann, P. (2005). Nuclear speckles and nucleoli targeting by PIP(2)-PDZ domain interactions. EMBO J. *24*, 2556–2565.

Nam, S.C., and Choi, K.W. (2003). Interaction of Par-6 and Crumbs complexes is essential for photoreceptor morphogenesis in Drosophila. Development *130*, 4363–4372.

Nicholls, A. (1992). GRASP: Graphical Representation and Analysis of Surface Properties (New York: Columbia University).

Nishimura, T., Yamaguchi, T., Kato, K., Yoshizawa, M., Nabeshima, Y., Ohno, S., Hoshino, M., and Kaibuchi, K. (2005). PAR-6-PAR-3 mediates Cdc42-induced Rac activation through the Rac GEFs STEF/Tiam1. Nat. Cell Biol. *7*, 270–277.

Pinal, N., Goberdhan, D.C., Collinson, L., Fujita, Y., Cox, I.M., Wilson, C., and Pichaud, F. (2006). Regulated and polarized PtdIns(3,4,5)P3 accumulation is essential for apical membrane morphogenesis in photoreceptor epithelial cells. Curr. Biol. *16*, 140–149.

Plant, P.J., Fawcett, J.P., Lin, D.C., Holdorf, A.D., Binns, K., Kulkarni, S., and Pawson, T. (2003). A polarity complex of mPar-6 and atypical PKC binds, phosphorylates and regulates mammalian Lgl. Nat. Cell Biol. *5*, 301–308.

Sasaki, A.T., Chun, C., Takeda, K., and Firtel, R.A. (2004). Localized Ras signaling at the leading edge regulates PI3K, cell polarity, and directional cell movement. J. Cell Biol. *167*, 505–518.

Shi, S.H., Jan, L.Y., and Jan, Y.N. (2003). Hippocampal neuronal polarity specified by spatially localized mPar3/mPar6 and PI 3-kinase activity. Cell *112*, 63–75.

Suzuki, A., and Ohno, S. (2006). The PAR-aPKC system: lessons in polarity. J. Cell Sci. *119*, 979–987.

Suzuki, A., Yamanaka, T., Hirose, T., Manabe, N., Mizuno, K., Shimizu, M., Akimoto, K., Izumi, Y., Ohnishi, T., and Ohno, S. (2001). Atypical protein kinase C is involved in the evolutionarily conserved par protein complex and plays a critical role in establishing epithelia-specific junctional structures. J. Cell Biol. *152*, 1183–1196.

Tabuse, Y., Izumi, Y., Piano, F., Kemphues, K.J., Miwa, J., and Ohno, S. (1998). Atypical protein kinase C cooperates with PAR-3 to establish embryonic polarity in Caenorhabditis elegans. Development *125*, 3607–3614.

Vanhaesebroeck, B., Jones, G.E., Allen, W.E., Zicha, D., Hooshmand-Rad, R., Sawyer, C., Wells, C., Waterfield, M.D., and Ridley, A.J. (1999). Distinct PI(3)Ks mediate mitogenic signalling and cell migration in macrophages. Nat. Cell Biol. *1*, 69–71.

von Stein, W., Ramrath, A., Grimm, A., Muller-Borg, M., and Wodarz, A. (2005). Direct association of Bazooka/PAR-3 with the lipid phosphatase PTEN reveals a link between the PAR/aPKC complex and phosphoinositide signaling. Development *132*, 1675–1686.

Wang, F., Herzmark, P., Weiner, O.D., Srinivasan, S., Servant, G., and Bourne, H.R. (2002). Lipid products of PI(3)Ks maintain persistent cell polarity and directed motility in neutrophils. Nat. Cell Biol. *4*, 513–518.

Yan, J., Wen, W., Xu, W., Long, J.F., Adams, M.E., Froehner, S.C., and Zhang, M. (2005). Structure of the split PH domain and distinct lipid-binding properties of the PH-PDZ supramodule of alpha-syntrophin. EMBO J. *24*, 3985–3995.

Yu, J.W., Mendrola, J.M., Audhya, A., Singh, S., Keleti, D., DeWald, D.B., Murray, D., Emr, S.D., and Lemmon, M.A. (2004). Genome-wide analysis of membrane targeting by S. cerevisiae pleckstrin homology domains. Mol. Cell *13*, 677–688.

Zhang, H., and Macara, I.G. (2006). The polarity protein PAR-3 and TIAM1 cooperate in dendritic spine morphogenesis. Nat. Cell Biol. *8*, 227–237.

Zimmermann, P., Meerschaert, K., Reekmans, G., Leenaerts, I., Small, J.V., Vandekerckhove, J., David, G., and Gettemans, J. (2002). PIP(2)-PDZ domain binding controls the association of syntenin with the plasma membrane. Mol. Cell *9*, 1215–1225.

Accession Numbers

The atomic coordinates of Par-3 PDZ2 have been deposited in the Protein Data Bank (accession code 2OGP).